Biochemical and Biophysical Research Communications 460 (2015) 82–87

Contents lists available at ScienceDirect

Biochemical and Biophysical Research Communications

journal homepage: www.elsevier.com/locate/ybbrc

Apoptosis induction-related cytosolic calcium responses revealed by the dual FRET imaging of calcium signals and caspase-3 activation in a single cell

Akitoshi Miyamoto [a, b], Hiroshi Miyauchi [c], Takako Kogure [d], Atsushi Miyawaki [d], Takayuki Michikawa [a, e, f, **], Katsuhiko Mikoshiba [a, *]

[a] Laboratory for Developmental Neurobiology, RIKEN Brain Science Institute, Wako, Saitama 351-0198, Japan
[b] Division of Neuronal Network, Department of Basic Medical Sciences, Institute of Medical Science, The University of Tokyo, Minato-ku, Tokyo 108-8639, Japan
[c] Saitama Medical University Hospital, Iruma, Saitama 350-0495, Japan
[d] Laboratory for Cell Function Dynamics, RIKEN Brain Science Institute, Wako, Saitama 351-0198, Japan
[e] Brain Science Institute, Saitama University, 255 Shimo-Okubo, Sakura-ku, Saitama 338-8570, Japan
[f] Laboratory for Behavioral Genetics, RIKEN Brain Science Institute, 2-1 Hirosawa, Wako, Saitama 351-0198, Japan

ARTICLE INFO

Article history:
Received 9 February 2015
Available online 18 May 2015

Keywords:
Calcium imaging
Apoptosis
Caspase
FRET
Biosensors

ABSTRACT

Stimulus-induced changes in the intracellular Ca^{2+} concentration control cell fate decision, including apoptosis. However, the precise patterns of the cytosolic Ca^{2+} signals that are associated with apoptotic induction remain unknown. We have developed a novel genetically encoded sensor of activated caspase-3 that can be applied in combination with a genetically encoded sensor of the Ca^{2+} concentration and have established a dual imaging system that enables the imaging of both cytosolic Ca^{2+} signals and caspase-3 activation, which is an indicator of apoptosis, in the same cell. Using this system, we identified differences in the cytosolic Ca^{2+} signals of apoptotic and surviving DT40 B lymphocytes after B cell receptor (BCR) stimulation. In surviving cells, BCR stimulation evoked larger initial Ca^{2+} spikes followed by a larger sustained elevation of the Ca^{2+} concentration than those in apoptotic cells; BCR stimulation also resulted in repetitive transient Ca^{2+} spikes, which were mediated by the influx of Ca^{2+} from the extracellular space. Our results indicate that the observation of both Ca^{2+} signals and cells fate in same cell is crucial to gain an accurate understanding of the function of intracellular Ca^{2+} signals in apoptotic induction.

1. Introduction

Ca^{2+} acts as an intracellular messenger, relaying information that regulates many cellular responses, such as transcription factor activation [1,2], and cell fate decisions [3,4]. To control these diverse cellular processes, Ca^{2+} signals have evolved to be highly variable in their amplitude, frequency, and duration [5].

Extracellular stimulation causes intracellular Ca^{2+} changes that control apoptotic cell death [6,7]. The relationship between these changes in the cytosolic Ca^{2+} concentration and apoptosis have long been debated, based on the analyses of intracellular Ca^{2+} signals and apoptotic cell death that were performed separately [8–10]. Therefore the one-to-one correlation between the Ca^{2+} signals and apoptosis at the single-cell level has never been confirmed. For understand the functional roles of intracellular Ca^{2+} signaling during the induction of apoptosis, observation of both Ca^{2+} signals and cell fates in the same cell after apoptotic stimulation is absolutely necessary, because of cell-to-cell variations in the temporal pattern of intracellular Ca^{2+} changes [11] and cell fates after apoptotic stimuli [12,13].

2. Materials and methods

2.1. Dual FRET imaging using RACS3 and YC3.60

Imaging of yellow cameleon 3.60 (YC3.60) [14] and RACS3 signals was performed with a confocal laser microscope A1 (Nikon)

** Corresponding author. Brain Science Institute, Saitama University, 255 Shimo-Okubo, Sakura-ku, Saitama 338-8570, Japan.
* Corresponding author. Laboratory for Developmental Neurobiology, RIKEN Brain Science Institute, 2-1 Hirosawa, Wako, Saitama 351-0198, Japan.
E-mail addresses: t-michikawa@brain.riken.jp (T. Michikawa), mikosiba@brain.riken.jp (K. Mikoshiba).

http://dx.doi.org/10.1016/j.bbrc.2015.02.045
0006-291X/

with a 60 × objective (NA 1.42, Nikon), excitation with a laser diode (440 nm) and a dichroic mirror of 457 nm. The imaging conditions were optimized in the previous study [15]. Fluorescent signals were detected with 32 PMTs. Each PMT had a 6 nm bandwidth, and the ranges of 460–514 nm, 514–556 nm, 556–610 nm and 610–652 nm were used for the acquisition of signals of ECFP, Venus, dKeima570 and FP615, respectively. For imaging of cytosolic Ca^{2+} changes and caspase-3 activation in the same cells, ECFP and Venus signals from YC3.60 and RACS3-expressing DT40 cells were acquired every 5 s for the first 60 min, and then dKeima570 and FP615 signals were acquired every 10 min for 14 h. Acquisition was performed with NIS-Elements (Nikon). Venus/ECFP emission ratio of YC3.60 and dKeima570/FP615 emission ratio of RACS3 were defined as R, and ΔR was defined as R-R_0 where R_0 is the basal level of R before M4 antibody addition.

Descriptions of other methods are provided in the Supplementary Materials.

3. Results and discussion

3.1. The temporal pattern of Ca^{2+} signals in BCR-stimulated DT40 cells at physiological temperature

B cell receptor (BCR) stimulation with the anti-BCR antibody M4 [16] induces a rapid increase in free cytoplasmic Ca^{2+} because of the production of IP_3, which is followed by the release of Ca^{2+} from the intracellular Ca^{2+} stores [17] and brings about apoptotic cell death in DT40 cells, an avian leucosis chicken pre-B cell line [18,4]. We confirmed that M4 stimulation induced apoptosis in 27.1 ± 5% of DT40 cells cultured at 39.5 °C 15 h after stimulation by flow cytometric analysis (Fig. 1A and B). Surprisingly, at room temperature (25 °C) the proportion of sub-G1 stage cells undergoing apoptotic cell death was significantly smaller than the proportion undergoing cell death at 39.5 °C (Fig. 1A and B), indicating that BCR induced apoptotic cell death is inhibited at room temperature, at least within 15 h of BCR stimulation.

This result provides direct evidence that the observation of the cytosolic Ca^{2+} response at physiological temperatures is indispensable for the precise understanding of the functional role of Ca^{2+} signals during the induction of apoptosis. Therefore, in this study, we used a genetically-encoded Ca^{2+} indicator: yellow cameleon 3.60 (YC3.60), for the long-term recording of Ca^{2+} concentrations at the culture temperature (39.5 °C). YC3.60 is a ratiometric Ca^{2+} sensor, which permits quantitative measurement of Ca^{2+} concentration that can eliminate the artifacts caused by indicator concentration and cell thickness or movement. Measurements using YC3.60 are based on the fluorescence resonance energy transfer (FRET) between the ECFP and the enhanced yellow fluorescent protein Venus [19].

The cytosolic YC3.60 signals in a single DT40 cell stimulated by 10 μg/ml of M4 were recorded at 0.2 Hz at 39.5 °C for 1 h. BCR stimulation typically induced large initial increases in Ca^{2+} concentration, which were cell-to-cell variations in the oscillatory Ca^{2+} responses following the large Ca^{2+} concentration increase (Fig. 1C). We confirmed that knockdown of all three types of IP_3R significantly inhibited BCR-induced apoptotic cell death and resulted in the loss of these initial Ca^{2+} spikes as well as the subsequent Ca^{2+} signals at 39.5 °C (Fig. 1C), as was shown in previous study at 25 °C [4]. These results suggest that YC3.60 faithfully reports BCR-stimulation-induced Ca^{2+} signals, which are related to cell fate decisions [4] at 39.5 °C.

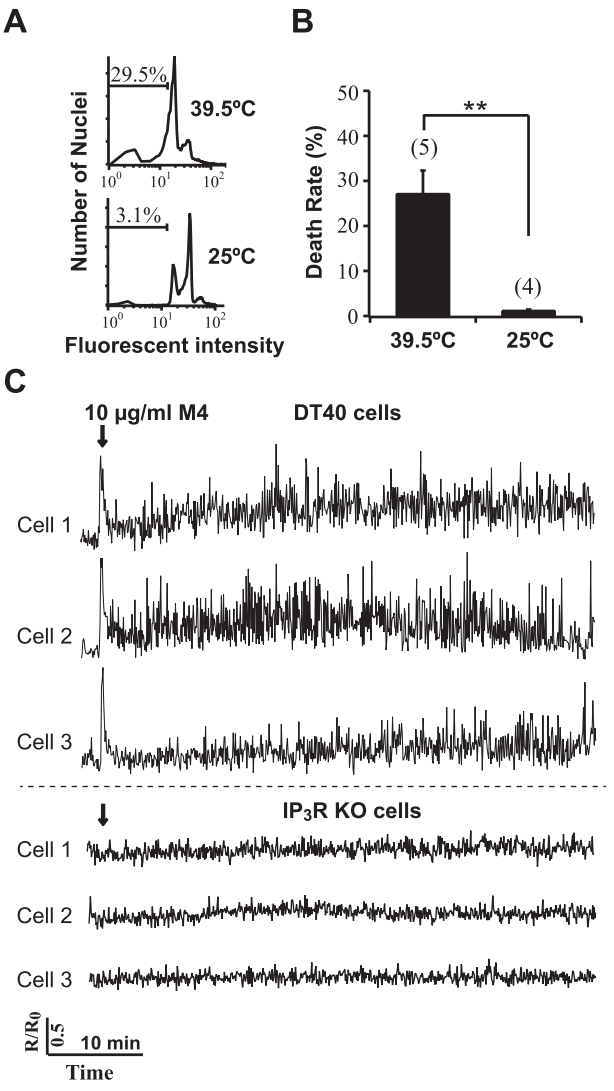

Fig. 1. Temperature-dependent cell viability and Ca^{2+} signals at physiological temperature after BCR-stimulation. (A) Flow cytometric analysis of the apoptosis of DT40 cells treated with M4 for 15 h at 39.5 °C (top) or 25 °C (bottom). The apoptotic cell death rate, as detected by a fluorescent intensity less than 150, is shown. (B) The mean of the fraction of apoptotic cell death rate after the addition of 10 μg/mL M4 for 15 h. The total number of measurements analyzed is given in parentheses. **: $p < 0.01$; Student's *t*-test. Error bars represent standard deviation (SD). (C) Representative traces of Ca^{2+} responses, as monitored by the ratio change of YC3.60 fluorescence in wild-type DT40 cells and DT40 cells lacking all three types of IP_3R (IP_3R KO cells), after the application of 10 μg/mL M4 (arrow) at 39.5 °C.

3.2. Development of a novel activated caspase-3 sensor

To identify the pattern of Ca^{2+} signals that is associated with apoptosis, cell fate tracking after Ca^{2+} imaging is essential. SCAT3, a sensor of activated caspase-3 [20], has been used to detect apoptosis with single-cell resolution [21,22]. However, because SCAT3 also uses ECFP and Venus as a FRET donor and acceptor, respectively, SCAT3 cannot be used with the YC3.60 fluorescent sensor that is suitable for long-term Ca^{2+} imaging at physiological temperature.

To overcome this problem, we improved the fluorescent properties of monomeric red fluorescent protein1 (mRFP1) by inserting several point mutations, and developed a novel pair of fluorescent proteins to sense caspase-3 activation. Fig. 2A shows the amino acid sequence of a modified fluorescent protein whose maximal emission intensity can be observed at 615 nm (Fig. 2B), while the emission intensity of its ancestor protein, mRFP1, can be observed at approximately 607 nm [23]. The modified protein,

FP615, possessed an improved extinction coefficient (Table S1) and was suitable for use as a FRET acceptor in combination with dKeima570 [24] as a FRET donor (Fig. 2B). Using this pair of fluorescent proteins, we have developed a red activated caspase-3 sensor (RACS3) composed of two FP615 proteins (Td FP615), a dKeima570 protein and a linker sequence containing a site that is cleavable by caspase-3: aspartic acid (D) – glutamic acid (E) – valine (V) – aspartic acid (D) DEVD. (Fig. 2C and D).

When the RACS3 protein was purified from *E. coli* and incubated with active caspase-3 in vitro, the ratio of fluorescence intensity at 570 nm and 615 nm was greatly increased (from 0.75 ± 0.02 to 1.83 ± 0.01, n = 3) (Fig. 2E). RACS3 was cleaved into two fragments by treatment with activated caspase-3, while the fluorescence intensity of the RACS3(DEVG) protein, in which the second aspartic acid (D) in the caspase-3 cleavage site was substituted with glycine (G), was unchanged by treatment with activated caspase-3 (Fig. S1A). These results indicate that RACS3 is specifically cleaved by caspase-3 and that the FRET signal of RACS3 can be used to detect the activation of caspase-3.

3.3. Optical detection of apoptosis using RACS3

We next established stable DT40 cell lines expressing both RACS3 and YC3.60 in order to monitor apoptotic induction and changes in the cytosolic Ca^{2+} concentration in the same cells. We monitored signals from the four fluorescent proteins simultaneously in this cell line using 32 PMTs (Fig. S1F). To confirm that apoptotic cell death can be detected in living DT40 cells, we first monitored the RACS3 signal from each cell every 10 min for 14 h after BCR stimulation. The RACS3 ratio (dKeima570/FP615) increased with a mean of 28 ± 6% (n = 67) (Fig. 2F), only once for each cell during the recording period. Indeed, the RACS3 signals changes were accompanied by DNA fragmentation (Fig. S1B), and the amount of cleaved RACS3 in this DT40 cell line increased after M4 stimulation (Fig. S1C). The timing of the RACS3 signal changes due to FRET varied from cell to cell, and RACS3 fluorescence ratio increases of more than 0.15 were most frequently observed 6 h after stimulation and lasted for 14 h (Fig. 2G). In contrast, we did not detect any cleavage (Fig. S1C) or FRET changes in the RACS3(DEVG) protein (Fig. 2F) for at least 14 h. The expression of RACS3 did not affect the fraction of cells that underwent apoptosis (Fig. S1D and E). These results demonstrate that RACS3 can be used to detect apoptotic cell death in living cells.

We found that the dKeima570 signal slightly increased when the YC3.60 signal changed in response to BCR stimulation (Fig. S1G). This finding may be caused by crosstalk between the Venus and dKeima570 fluorescents because their temporal patterns were almost the same (Fig. S1G). However, the ratio between the emissions from the dKeima570 and FP615 proteins of RACS3 was almost constant, even when the YC3.60 signal was increased to 150% in response to increases in the Ca^{2+} concentration (Fig. S1H), suggesting that the effect of crosstalk from Venus to dKeima570 was negligible. From these results, we concluded that the dual imaging system, which allowed us to monitor both cytosolic Ca^{2+} signals and caspase-3 activation in same cell, was functional.

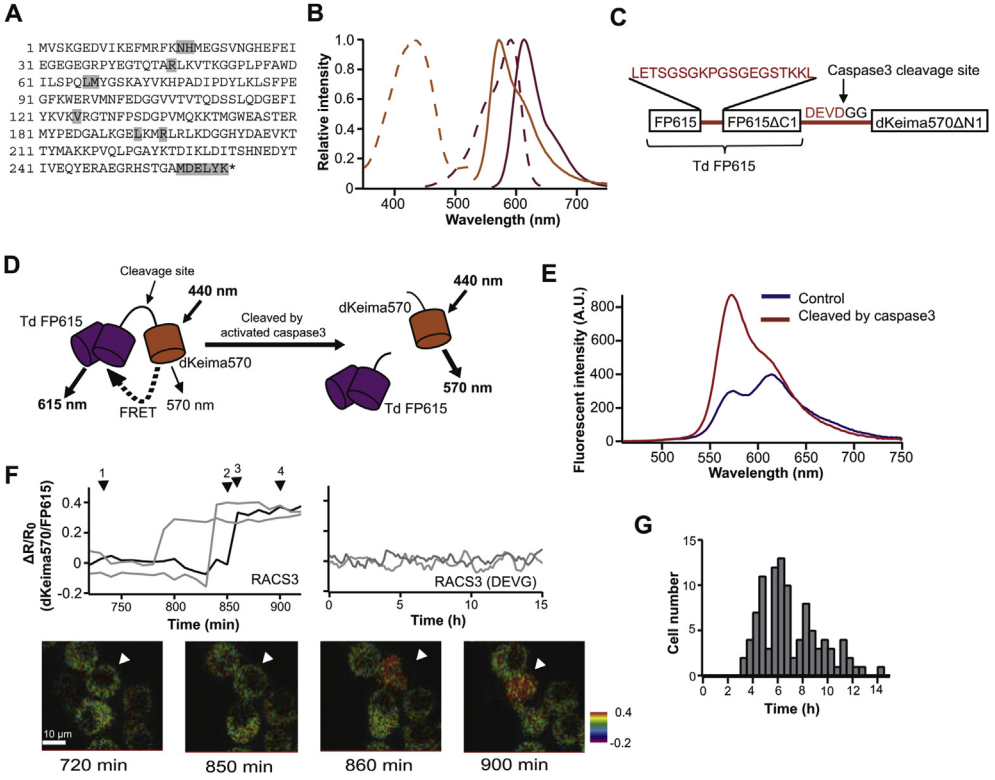

Fig. 2. Development of a novel activated caspase-3 sensor RACS3. (A) Amino acid sequence of FP615. Amino acid residues that have been mutated from those of the ancestral protein, mRFP1, are indicated by the gray boxes. (B) The excitation (broken line) and emission (continuous line) spectra of dKeima570 (orange) and FP615 (purple). (C) The basic design of RACS3 (for ΔC1 and ΔN1, see the Materials and Methods section). (D) A schematic representation of RACS3. (E) The emission spectra of purified RACS3 before (blue) and after (red) treatment with active caspase-3 for 2 h, as detected by a spectrofluorometer. (F) RACS3 and RACS3(DEVG) signals in DT40 cells that were stimulated with 10 μg/mL M4 at 39.5 °C. Data from three different cells are shown for each construct. Images of the cells, represented by a black line, are shown at the bottom (white arrowheads) of the figure. Images of the cells at times, 1–4 after M4 application, which are indicated in the upper graph, are shown (black arrowheads). (G) A histogram of the time required for caspase-3 activation, as monitored with RACS3 in the presence of 10 μg/mL M4.

3.4. Comparison of Ca^{2+} dynamics between apoptotic and surviving cells

To characterize the Ca^{2+} signals that are associated with the induction of apoptosis, we compared the Ca^{2+} signals in apoptotic cells with those in surviving cells during the first 1 h after BCR stimulation. Cells exhibiting an increase in the RACS3 signal ratio that was larger than 0.15 during the 14 h after the onset of BCR stimulation were designated as apoptotic cells. BCR stimulation evoked a biphasic Ca^{2+} signaling response in both apoptotic and surviving cells; the first component of this response was the initial large Ca^{2+} spikes when M4 was applied, and the second was the sustained elevation of the Ca^{2+} concentration that was accompanied by repetitive Ca^{2+} transient fluctuations in the Ca^{2+} concentration (Fig. 3A). The sustained elevations of the Ca^{2+} concentrations with repetitive Ca^{2+} fluctuations were also observed using high frequency measurements (0.5 Hz) at 39.5 °C (Fig. S2), suggesting that the sustained Ca^{2+} elevation is not an artifact of the low-frequency recording.

We found that the total cumulative amount (the area under the curve) of Ca^{2+} responses induced by BCR-stimulation in the apoptotic cells was smaller than the amount induced in the surviving cells (Fig. 3B). The peak amplitude (Fig. 3C) and the number of fluctuations in Ca^{2+} concentration per minute (Fig. 3D) in apoptotic cells was significantly smaller than those in surviving cells. To quantify the amount of sustained Ca^{2+} elevation that were accompanied by repetitive fluctuations in Ca^{2+} concentrations, Ca^{2+} traces were smoothed with a moving average (Eq. (1), see the Supplementary Materials) and the plateau level was estimated by fitting the trace with a single exponential function (Eq. 2, see the Supplementary Materials). The plateau level of apoptotic cells was significantly smaller than the level of surviving cells (Fig. 3F). However, the baseline levels of cytosolic Ca^{2+} before stimulation were not significantly different in apoptotic and surviving cells (Fig. S3). These results indicate that the amplitude and the frequency of the Ca^{2+} signals are associated with the induction of apoptosis, and that the cells in which BCR stimulation evoked larger Ca^{2+} responses have a tendency to survive after BCR stimulation. These results were consisted with the previous study [25,26].

To analyze the source of the Ca^{2+} signals, we monitored changes in the cytosolic Ca^{2+} concentration after BCR stimulation in the absence of extracellular Ca^{2+} (Fig. 4A). The presence or absence of extracellular Ca^{2+} did not affect the amplitude of the initial Ca^{2+} spikes (Fig. 4B), suggesting that the initial Ca^{2+} spikes are generated by the release of Ca^{2+} from intracellular Ca^{2+} stores. In contrast, the sustained Ca^{2+} elevation with repetitive Ca^{2+} spikes that followed the initial Ca^{2+} spike was markedly reduced by eliminating the extracellular Ca^{2+} (Fig. 4A). The plateau level of the cytosolic Ca^{2+} concentration was significantly reduced in the absence of extracellular Ca^{2+} (Fig. 4C). These results indicate that a Ca^{2+} influx is involved in the generation of the sustained Ca^{2+} elevation with repetitive Ca^{2+} spikes.

In apoptotic cells, BCR stimulation induced smaller intracellular Ca^{2+} responses. However, both BCR-induced Ca^{2+} responses and apoptotic cell death are inhibited in the DT40 cells lacking all three types of IP_3R [4], and we confirmed that both the M4-induced

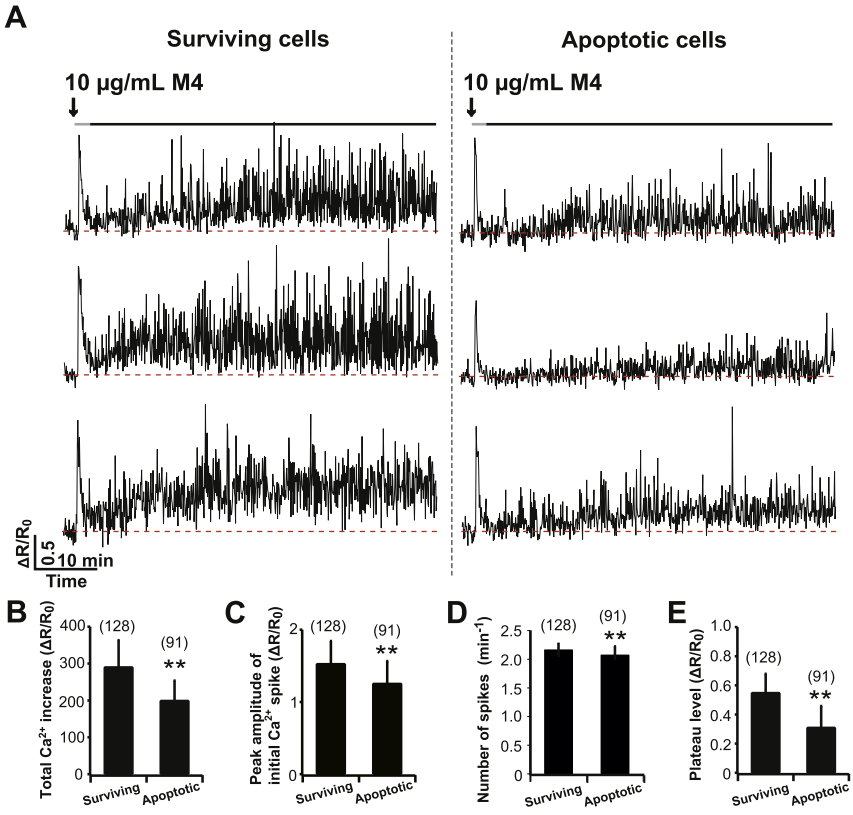

Fig. 3. Comparison of the temporal pattern of cytosolic Ca^{2+} changes in apoptotic and surviving cells. (A) Typical patterns of the single-cell Ca^{2+} increase that is induced by M4 treatment in apoptotic and surviving cells. YC3.60 signals from three different cells are shown for each cell category. M4 application is indicated by the arrow, and red broken lines represent the baseline of the YC3.60 signal ratio. The grey and black lines indicate the initial Ca^{2+} spikes and the subsequent sustained elevation in Ca^{2+} concentration with repetitive Ca^{2+} fluctuation, respectively. (B) The total Ca^{2+} increase calculated as the area under the curve of the Ca^{2+} signals following 1 h of M4 application. (C) The peak amplitudes of the initial Ca^{2+} spikes. (D) The number of Ca^{2+} spikes per minutes. (E) The plateau level as estimated from a single exponential function fitted to the smoothed Ca^{2+} signals. The total number of cells analyzed is given in parentheses. **: $p < 0.01$; n.s.: not significant, Student's t-test in B-E. Value and error bars represent the mean and SD, respectively in B-E.

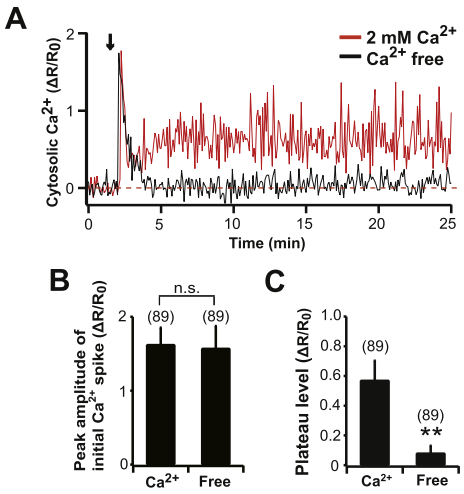

Fig. 4. The effects of extracellular Ca^{2+} concentration on the changes in cytosolic Ca^{2+} concentration that are induced by BCR stimulation. (A) Representative changes in cytosolic Ca^{2+} levels, as measured with YC3.60, in the presence (red) and absence of extracellular Ca^{2+} (black), in cells stimulated with 10 μg/mL M4 at 39.5 °C. The application of M4 is indicated by the arrow. (B) The peak amplitude of the initial Ca^{2+} spikes. (C) Plateau levels, as estimated from a single exponential function fitted to the smoothed Ca^{2+} signals. The total number of cells analyzed is given in parentheses. Error bars represent SD. (B, C). **: $p < 0.01$; n.s.: not significant; Student's *t*-test (B, C).

initial Ca^{2+} spikes and the sustained elevation of the Ca^{2+} concentration were lost in this cell line. These results raise the possibility that BCR-induced cytosolic Ca^{2+} signals are essential for the initiation of apoptosis but that the levels of the intracellular Ca^{2+} responses that are induced by BCR stimulation is also one of the determinants of cell fate.

While previous studies mainly focused on the frequencies and amplitudes of the IP_3R-mediated Ca^{2+} release response after BCR-engagement [8,9], the physiological role of Ca^{2+} influx-dependent sustained Ca^{2+} elevation in cell fate decisions requires further investigation in future study. The molecular mechanism by which the Ca^{2+} signal pattern determines the fate of each cell remains to be elucidated. Recently, some cell-fate determinants, such as the level or states of the receptor proteins that regulate apoptosis [12] and the cell cycle stage at which the cell is exposed to apoptotic stimulus [13], have been reported; thus, there is a possibility that these cell-fate determinants modify the stimuli-induced intracellular Ca^{2+} signals to execute the processes that lead to the cells' fates.

This study provides novel insight into the pattern of the Ca^{2+} signals and apoptotic induction. The downstream elements that decode the intracellular Ca^{2+} signals that result in the induction of apoptosis or cell survival must be determined in future studies. Mitochondria and Ca^{2+}-dependent proteins, such as protein kinase C (PKC) [27], calcium/calmodulin-dependent protein kinase II (CaMKII) [28], and calpain [29], are promising candidates. Several fluorescent probes have been published during the last decade and are capable of monitoring mitochondrial Ca^{2+} signals [30] and the activity of Ca^{2+}-dependent proteins, including PKC [31], CaMKII [32], and calpain [33]. Dual imaging, specifically combining these fluorescent probes with RACS3 in single cell, will provide us with the entire picture of Ca^{2+}-dependent regulation of life-and-death decisions. Recent developments in dual FRET imaging systems [34–37] have enabled us to observe the interaction of signaling molecules in single cell and to clarify the physiological function of signaling molecules; the dual imaging system would be a pivotal tool for understanding the role of the signaling cascade in cellular processes.

In this study, we observed the BCR-induced cytosolic Ca^{2+} response for only 1 h to avoid complications created by the phototoxicity of the cells and the photobleaching of YC3.60. However, in future studies, the observation of intracellular Ca^{2+} signals from simulation to cell death will also be necessary for a precise understanding of the functional role of Ca^{2+} signaling in apoptosis induction.

In summary, this study suggests that observing the one-to-one correlation between signaling molecules at the single cell level is essential to obtain a better understanding of regulatory mechanisms of cellular processes and that monitoring multiple biological parameters in an individual cell would allow for the analysis of complex signal transduction networks.

Conflict of interest

None.

Acknowledgments

We would like to thank Dr. M. Miura, Y. Baba, T. Kurosaki, and K. Hirose for fruitful discussions. We thank Nikon Instruments Inc. for technical support. We thank Dr. R.Y. Tsien for his gift of mRFP1 cDNA. We thank Dr. H. Nakamura for data analysis. We thank Dr. H. Ando, Dr. C. Hisatsune and Dr. H. Bannai for critically reading this manuscript. This work was supported by grants from the Ministry of Education, Culture, Sports, Science and Technology of Japan (20220007 to K.M. and 24500476 to T.M.).

Appendix A. Supplementary data

Supplementary data related to this chapter can be found at http://dx.doi.org/10.1016/j.bbrc.2015.02.045.

References

[1] R.E. Dolmetsch, K. Xu, R.S. Lewis, Calcium oscillations increase the efficiency and specificity of gene expression, Nature 392 (1998) 933–936.
[2] W. Li, J. Llopis, M. Whitney, G. Zlokarnik, R.Y. Tsien, Cell-permeant caged $InsP_3$ ester shows that Ca^{2+} spike frequency can optimize gene expression, Nature 392 (1998) 936–941.
[3] S. Feske, ORAI1 and STIM1 deficiency in human and mice: roles of store-operated Ca^{2+} entry in the immune system and beyond, Immunol. Rev. 231 (2009) 189–209.
[4] H. Sugawara, M. Kurosaki, M. Takata, T. Kurosaki, Genetic evidence for involvement of type 1, type 2 and type 3 inositol 1,4,5-trisphosphate receptors in signal transduction through the B-cell antigen receptor, EMBO J. 16 (1997) 3078–3088.
[5] M.J. Berridge, P. Lipp, M.D. Bootman, The versatility and universality of calcium signalling, Nat. Rev. Mol. Cell. Biol. 1 (2000) 11–21.
[6] A.M. Scharenberg, L.A. Humphries, D.J. Rawlings, Calcium signalling and cell-fate choice in B cells, Nat. Rev. Immunol. 7 (2007) 778–789.
[7] M.W. Harr, Y. Rong, M.D. Bootman, H.L. Roderick, C.W. Distelhorst, Glucocorticoid-mediated inhibition of Lck modulates the pattern of T cell receptor-induced calcium signals by down-regulating inositol 1,4,5-trisphosphate receptors, J. Biol. Chem. 284 (2009) 31860–31871.
[8] C. Li, X. Wang, H. Vais, C.B. Thompson, J.K. Foskett, C. White, Apoptosis regulation by Bcl-xL modulation of mammalian inositol 1,4,5-trisphosphate receptor channel isoform gating, Proc. Natl. Acad. Sci. U. S. A. 104 (2007) 12565–12570.
[9] E.F. Eckenrode, J. Yang, G.V. Velmurugan, J.K. Foskett, C. White, Apoptosis protection by Mcl-1 and Bcl-2 modulation of inositol 1,4,5-trisphosphate receptor-dependent Ca^{2+} signaling, J. Biol. Chem. 285 (2010) 13678–13684.
[10] C. White, C. Li, J. Yang, N.B. Petrenko, M. Madesh, C.B. Thompson, J.K. Foskett, The endoplasmic reticulum gateway to apoptosis by Bcl-$_X$L modulation of the $InsP_3R$, Nat. Cell. Biol. 7 (2005) 1021–1028.
[11] M. Prentki, M.C. Glennon, A.P. Thomas, R.L. Morris, F.M. Matschinsky, B.E. Corkey, Cell-specific patterns of oscillating free Ca^{2+} in carbamylcholine-stimulated insulinoma cells, J. Biol. Chem. 263 (1988) 11044–11047.
[12] S.L. Spencer, S. Gaudet, J.G. Albeck, J.M. Burke, P.K. Sorger, Non-genetic origins of cell-to-cell variability in TRAIL-induced apoptosis, Nature 459 (2009) 428–432.
[13] T. Hashimoto, K. Juso, M. Nakano, T. Nagano, S. Kambayashi, A. Nakashima, U. Kikkawa, S. Kamada, Preferential Fas-mediated apoptotic execution at G1

phase: the resistance of mitotic cells to the cell death, Cell. Death Dis. 3 (2012) e313.
[14] T. Nagai, S. Yamada, T. Tominaga, M. Ichikawa, A. Miyawaki, Expanded dynamic range of fluorescent indicators for Ca^{2+} by circularly permuted yellow fluorescent proteins, Proc. Natl. Acad. Sci. U. S. A. 101 (2004) 10554–10559.
[15] A. Miyamoto, H. Bannai, T. Michikawa, K. Mikoshiba, Optimal microscopic systems for long-term imaging of intracellular calcium using a ratiometric genetically-encoded calcium indicator, Biochem. Biophys. Res. Commun. 434 (2013) 252–257.
[16] C.L. Chen, J.E. Lehmeyer, M.D. Cooper, Evidence for an IgD homologue on chicken lymphocytes, J. Immunol. 129 (1982) 2580–2585.
[17] K. Mikoshiba, IP_3 receptor/Ca^{2+} channel: from discovery to new signaling concepts, J. Neurochem. 102 (2007) 1426–1446.
[18] S. Kim, E.H. Humphries, L. Tjoelker, L. Carlson, C.B. Thompson, Ongoing diversification of the rearranged immunoglobulin light-chain gene in a bursal lymphoma cell line, Mol. Cell. Biol. 10 (1990) 3224–3231.
[19] T. Nagai, K. Ibata, E.S. Park, M. Kubota, K. Mikoshiba, A. Miyawaki, A variant of yellow fluorescent protein with fast and efficient maturation for cell-biological applications, Nat. Biotechnol. 20 (2002) 87–90.
[20] K. Takemoto, T. Nagai, A. Miyawaki, M. Miura, Spatio-temporal activation of caspase revealed by indicator that is insensitive to environmental effects, J. Cell. Biol. 160 (2003) 235–243.
[21] E. Kuranaga, T. Matsunuma, H. Kanuka, K. Takemoto, A. Koto, K. Kimura, M. Miura, Apoptosis controls the speed of looping morphogenesis in Drosophila male terminalia, Development 138 (2011) 1493–1499.
[22] Y. Nakajima, E. Kuranaga, K. Sugimura, A. Miyawaki, M. Miura, Nonautonomous apoptosis is triggered by local cell cycle progression during epithelial replacement in Drosophila, Mol. Cell. Biol. 31 (2011) 2499–2512.
[23] L. Wang, W.C. Jackson, P.A. Steinbach, R.Y. Tsien, Evolution of new nonantibody proteins via iterative somatic hypermutation, Proc. Natl. Acad. Sci. U. S. A. 101 (2004) 16745–16749.
[24] T. Kogure, S. Karasawa, T. Araki, K. Saito, M. Kinjo, A. Miyawaki, A fluorescent variant of a protein from the stony coral Montipora facilitates dual-color single-laser fluorescence cross-correlation spectroscopy, Nat. Biotechnol. 24 (2006) 577–581.
[25] T. Higo, M. Hattori, T. Nakamura, T. Natsume, T. Michikawa, K. Mikoshiba, Subtype-specific and ER lumenal environment-dependent regulation of inositol 1,4,5-trisphosphate receptor type 1 by ERp44, Cell 120 (2005) 85–98.
[26] T. Higo, K. Hamada, C. Hisatsune, N. Nukina, T. Hashikawa, M. Hattori, T. Nakamura, K. Mikoshiba, Mechanism of ER stress-induced brain damage by IP_3 receptor, Neuron 68 (2010) 865–878.
[27] M.C. Turco, M.F. Romano, A. Petrella, R. Bisogni, P. Tassone, S. Venuta, NF-kappaB/Rel-mediated regulation of apoptosis in hematologic malignancies and normal hematopoietic progenitors, Leukemia 18 (2004) 11–17.
[28] K. Hughes, S. Edin, A. Antonsson, T. Grundstrom, Calmodulin-dependent kinase II mediates T cell receptor/CD3– and phorbol ester-induced activation of IkappaB kinase, J. Biol. Chem. 276 (2001) 36008–36013.
[29] A.K. Sharma, B. Rohrer, Calcium-induced calpain mediates apoptosis via caspase-3 in a mouse photoreceptor cell line, J. Biol. Chem. 279 (2004) 35564–35572.
[30] T. Nagai, A. Sawano, E.S. Park, A. Miyawaki, Circularly permuted green fluorescent proteins engineered to sense Ca^{2+}, Proc. Natl. Acad. Sci. U. S. A. 98 (2001) 3197–3202.
[31] J.D. Violin, J. Zhang, R.Y. Tsien, A.C. Newton, A genetically encoded fluorescent reporter reveals oscillatory phosphorylation by protein kinase C, J. Cell. Biol. 161 (2003) 899–909.
[32] K. Takao, K. Okamoto, T. Nakagawa, R.L. Neve, T. Nagai, A. Miyawaki, T. Hashikawa, S. Kobayashi, Y. Hayashi, Visualization of synaptic Ca^{2+}/calmodulin-dependent protein kinase II activity in living neurons, J. Neurosci. 25 (2005) 3107–3112.
[33] P.W. Vanderklish, L.A. Krushel, B.H. Holst, J.A. Gally, K.L. Crossin, G.M. Edelman, Marking synaptic activity in dendritic spines with a calpain substrate exhibiting fluorescence resonance energy transfer, Proc. Natl. Acad. Sci. U. S. A. 97 (2000) 2253–2258.
[34] H.W. Ai, K.L. Hazelwood, M.W. Davidson, R.E. Campbell, Fluorescent protein FRET pairs for ratiometric imaging of dual biosensors, Nat. Methods 5 (2008) 401–403.
[35] Y. Niino, K. Hotta, K. Oka, Simultaneous live cell imaging using dual FRET sensors with a single excitation light, PLoS One 4 (2009) e6036.
[36] W. Tomosugi, T. Matsuda, T. Tani, T. Nemoto, I. Kotera, K. Saito, K. Horikawa, T. Nagai, An ultramarine fluorescent protein with increased photostability and pH insensitivity, Nat. Methods 6 (2009) 351–353.
[37] D.M. Shcherbakova, M.A. Hink, L. Joosen, T.W. Gadella, V.V. Verkhusha, An orange fluorescent protein with a large stokes shift for single-excitation multicolor FCCS and FRET imaging, J. Am. Chem. Soc. 134 (2012) 7913–7923.